

Published in final edited form as:

*J Mol Biol.* 2011 July 1; 410(1): 27–38. doi:10.1016/j.jmb.2011.04.071.

## The biochemistry and fidelity of synthesis by the apicoplast genome replication DNA polymerase Pfpref from the Malaria parasite *Plasmodium falciparum*

Scott R. Kennedy<sup>1</sup>, Cheng-Yao Chen<sup>1</sup>, Michael W. Schmitt<sup>1</sup>, Cole N. Bower<sup>1</sup>, and Lawrence A. Loeb<sup>1,2,\*</sup>

<sup>1</sup>Department of Pathology, University of Washington at Seattle, Seattle, WA 98195

<sup>2</sup>Department of Biochemistry, University of Washington at Seattle, Seattle, WA 98195

### Abstract

*Plasmodium falciparum*, the major causative agent of human malaria contains three separate genomes. The apicoplast, an intracellular organelle contains a ~35kb circular DNA genome of unusually high A/T content (>86%) that is replicated by the nuclear encoded replication complex Pfpref. Herein, we have expressed and purified the DNA polymerase domain of Pfpref (KPom1) and measured its fidelity using a *LacZ* based forward mutation assay. In addition, we analyzed the kinetic parameters for the incorporation of both complementary and non-complementary nucleotides incorporation using KPom1 lacking the 3'→5' exonucleolytic activity. KPom1 exhibits a strongly biased mutational spectrum in which the T → C is the most frequent single-base substitution and differs significantly from the closely related *E. coli* DNA polymerase I (pol I). Using *E. coli* harboring a temperature sensitive pol I allele, we established that KPom1 can complement the growth defective phenotype at an elevated temperature. We propose that the error bias of KPom1 may be exploited in the complementation assay to identify nucleoside analogs that mimic this base-mispairing and preferentially inhibit apicoplast DNA replication.

### Keywords

Replication; Apicoplexan; plDNA; Pom1

### Introduction

*Plasmodium falciparum*, the infectious agent associated with most cases of malaria, is responsible for an estimated 5 million deaths annually throughout the world<sup>1</sup>. This infectious parasite contains a nuclear and mitochondrial genome, as well as a third, unique, genome encapsulated in an organelle termed the apicoplast. The apicoplast, thought to be derived from the secondary endocytosis of photosynthetic algae, is involved in a variety of biosynthetic pathways and is required for parasite survival. The apicoplast contains its own plastid derived, ~35kb closed circular double-stranded DNA genome (plDNA) that is replicated by a bidirectional theta mechanism and segregated into the daughter cells<sup>2;3</sup>. The

\*To whom correspondence should be addressed: laloeb@u.washington.edu, phone: (206)543-6015, fax: (206) 543-3967, address: Dept of Pathology, HSB K-072, Box 357705, 1959 Pacific St NE, Seattle, WA 98125-7705.

**Publisher's Disclaimer:** This is a PDF file of an unedited manuscript that has been accepted for publication. As a service to our customers we are providing this early version of the manuscript. The manuscript will undergo copyediting, typesetting, and review of the resulting proof before it is published in its final citable form. Please note that during the production process errors may be discovered which could affect the content, and all legal disclaimers that apply to the journal pertain.

genome encodes several subunits of rRNA and the accompanying ribosomal proteins, 25 species of tRNA, an RNA polymerase, and several open reading frames coding for chaperones, as well as other proteins of unknown function<sup>4</sup>.

The biochemical and cellular processes involved in plDNA replication are poorly understood; however, several proteins that are involved in DNA metabolic processes are encoded by the nuclear genome, synthesized in the cytoplasm and transported to the apicoplast. These include a bacterial-like gyrase, a DNA ligase, and several unclassified open reading frames that are homologous to DNA repair enzymes<sup>5; 6</sup>. Of these, the apicoplast gyrase is a known target for inhibition by the drug ciprofloxin, a major therapeutic agent for the treatment of malaria, suggesting that other enzymes involved in plDNA replication and maintenance may be a useful drug target<sup>7; 8; 9; 10</sup>.

Apicoplast DNA replication is catalyzed by the nuclear encoded apicoplast-targeted polyprotein, Pfpex, which is a large (2016aa), multifunctional, peptide that contains three distinct domains that exhibit DNA primase, DNA helicase, and DNA polymerase activities, respectively<sup>11</sup> (Fig. 1 A). The helicase and a primase segments are homologous to T7 bacteriophage helicase and primase proteins<sup>11</sup>. The third domain contains a DNA polymerase that is evolutionarily related to prokaryotic DNA polymerase I, an A-family polymerase, based on sequence homology. Similar to DNA polymerase  $\gamma$ , which is localized to the mitochondria, Pfpex is believed to be the only DNA synthesizing enzyme in the apicoplast and is thought to be involved in DNA replication, repair, and recombination.

The three genomes present in *P. falciparum* (i.e. nuclear, mitochondrial, and plastidial) are among the most A/T rich yet sequenced, with the plDNA being the highest (86.9% A/T)<sup>4</sup>. Given the highly biased sequence composition of the apicoplast genome, we asked if the plDNA polymerase preferentially incorporated dATP and/or dTTP and thus has a role in the maintenance of the A/T rich genome. To this end, we have expressed and purified the DNA polymerase domain of Pfpex (henceforth referred to as KPom1, where KPom is shorthand for Klenow-like polymerase of malaria) and determined the frequencies of mis-incorporations and the effects of neighboring nucleotides using the M13mp2 forward mutation assay for KPom1 with and without a 3'→5' exonucleolytic activity. In addition, we also characterized the kinetics of incorporation of complementary and non-complementary nucleotide incorporation. Interestingly, we find that KPom1 exhibits a strongly biased error spectrum with the T→C single-base substitution being the most frequent and thus does not account for the maintenance of the A/T rich plastid genome. Even though the catalytic site motifs are highly conserved between *E. coli* Pol I and KPom1, the spectrum of mis-incorporation by KPom1 is markedly different from that of *E. coli* Pol I. This finding suggests that residues outside of the active site motifs may influence the fidelity of these two enzymes. Despite these differences, we established that KPom1 is able to substitute for *E. coli* Pol I, *in vivo*. We suggest that the error bias of KPom1 may be exploited in the complementation assay to identify nucleoside analogs that mimic base-mispairing and preferentially inhibit plDNA replication.

## Methods and Materials

### Construction of Recombinant Plasmids

The pSH576-derivative plasmids pECpolI and pECpol I-3'exo<sup>-</sup> that carry the *E. coli* wild-type and 3'→5' exonuclease-deficient pol I gene, respectively, were constructed as described previously<sup>12</sup>. The synthetic codon-optimized KPom1 or exonuclease deficient KPom1<sup>D1531A</sup> (KPom1<sup>exo-</sup>) genes (The amino acid numbering system is based on full length Pfpex) (Integrated DNA Technologies, Coralville, IA) (Supplemental Fig. S1) were cloned into the pMAL-c2X expression plasmid using the BamHI and HindIII sites. The

pMAL-c2X vector encodes a maltose-binding protein moiety, which was fused to the polymerase gene to expedite purification.

### Protein Expression and Purification

*E. coli* Rosetta2 cells (Novagen, EMD Chemicals) containing a pMAL-c2X-KPom1 plasmid were grown at 37 °C in 3 L of LB medium containing 50 µg/mL carbenicillin and 30 µg/mL chloramphenicol. Protein expression was induced by the addition of 0.2 mM IPTG at  $OD_{600} = \sim 0.6$ . Cells were grown for an additional 20 h at 21 °C and harvested by centrifugation. Cell pellets were resuspended in 30 mL Buffer A [20 mM Tris-HCl (pH 7.4), 1 mM DTT, 1 mM EDTA, 5% (w/v) glycerol, 2 mM benzamidine, 500 µg/mL lysozyme and 1 mM PMSF] +200 mM NaCl and incubated on ice for 1 h. The crude cell extract was sonicated and clarified by centrifugation at 15,000 ×g for 20 min (Supplemental Figure 2, Lane I). The supernatant was diluted with Buffer A+200 mM NaCl to 50 mL and loaded onto an amylose column pre-equilibrated in Buffer A. The column was then washed with 100 mL of Buffer A +200 mM NaCl. KPom1 was eluted with 20 mL of Buffer A+200 mM NaCl+20 mM maltose (Supplemental Figure 2, Lane II). The fractions containing KPom1 were pooled and directly diluted with an equal volume of Buffer A without NaCl and loaded onto a heparin column pre-equilibrated in Buffer A+100 mM NaCl. The column was washed with 40 mL of the same buffer. KPom1 was eluted with 30 mL of Buffer A+1M NaCl. Column fractions (2 mL each) containing fusion MBP-KPom1 protein were pooled and dialyzed at 4 °C overnight against the Factor Xa cleavage buffer [20 mM Tris-HCl (pH 8.0), 2 mM CaCl<sub>2</sub> and 100 mM NaCl] and then concentrated using an Amicon filter unit (MW cut-off 30,000 Da). The maltose-binding domain was cleaved by addition of Factor Xa per the manufacturer's protocol (New England Biolabs). After cleavage, the sample was diluted with four volumes of Buffer A and loaded onto an amylose column equilibrated with Buffer A. The column was then washed with 15 mL of Buffer A. The column flow-through (Supplemental Figure 2, Lane III) was directly diluted with an equal volume of Buffer A without NaCl and loaded on a heparin column pre-equilibrated in Buffer A+100 mM NaCl and washed with 20 mL of the same buffer. KPom1 was eluted with 15 mL of Buffer A+1M NaCl. Column fractions (1 mL) containing KPom1 proteins were pooled and dialyzed at 4 °C overnight against enzyme storage buffer [20 mM Tris-HCl (pH 7.4), 1 mM DTT, 0.5 mM EDTA, 50 mM NaCl, 2 mM benzamidine, 15% (w/v) glycerol] and concentrated using an Amicon filter unit (MW cut-off 30,000 Da) (Supplemental Figure 2, Lane IV). The mutant KPom1<sup>exo-</sup> protein was purified with the same protocol as the wild-type KPom1 preparation.

### Two-plasmid Based β-lactamase Reversion Assay

The assay was performed as described previously<sup>12</sup>. Briefly, the pol I<sup>ts</sup> *E. coli* strain JS200 (*SC-18 recA718 polA12 uvrA155 trpE65 lon-11 sulA1*) harboring the reporter plasmid pLA230 was transformed with plasmids encoding the gene for either wild-type pol I, pol I<sup>exo-</sup>, KPom1, or KPom1<sup>exo-</sup>. The recombinant strains were cultured at 30°C for 18 h in LB broth containing 30 mg/ml kanamycin, 12.5 mg/ml tetracycline, and 30 mg/ml chloramphenicol. A 0.01 volume of the pre-cultured broth was inoculated into fresh growth media, then cultured at 37 °C until an  $A_{600}$  of 1.0 was attained. Cells were then plated onto pre-warmed 2xYT agar plates supplemented with 30 µg/ml kanamycin, 12.5 µg/ml tetracycline, and 30 µg/ml chloramphenicol in the presence or absence of 100 µg/ml carbenicillin. After incubation at 37 °C for 24 h, colonies were counted, and reversion frequencies were calculated as the ratio of carbenicillin-resistant to total colonies.

### Genetic Complementation Assay

The spiral assay for testing genetic complementation of by exogenously expressed *E. coli* pol I and KPom1 DNA polymerases was conducted as described previously using the temperature sensitive *E. coli* strain JS200<sup>13</sup> To quantitatively determine the

complementation efficiency of pol I<sup>ts</sup> cells by wild-type and KPom1 DNA polymerases, ~1,000 cells of JS200 harboring either pHSG576, pEC-polI, pHSG576-KPom1, or pHSG576-KPom1<sup>D1798A</sup>, a mutant lacking polymerase activity, were plated on 2xYT agar plates containing tetracycline and chloramphenicol at 30 °C or 37 °C. The complementation efficiency of each construct was determined as the ratio of viable colonies at 37 °C on 2xYT agar plates relative to those at 30 °C plates after the 24 h incubation<sup>12</sup>. The results shown in all figures represent the average of three experiments that were carried out independently.

### Polymerase Activity Assays

The DNA polymerase activity of all purified proteins was quantified using activated calf thymus DNA, as previously described<sup>12</sup>. KPom1 and KPom1<sup>exo-</sup> protein were assayed for 3'-5' exonuclease activity using a duplex 5'-[<sup>32</sup>P]-labeled 27/36-mer DNA containing a 3' terminal G:G mismatch. Reaction mixtures (10 µL) contained 10 nM of 5'-[<sup>32</sup>P]-labeled 27/36-mer DNA and 0.01 units of wild-type Klenow fragment (New England Biolabs), exonuclease-deficient Klenow fragment (New England Biolabs), 20 nM KPom1, or KPom1<sup>exo-</sup> protein in the appropriate reaction buffer. Reactions were incubated at 37 °C for 15 min, and then terminated by addition of 10 µL of 2× gel loading buffer (100% formamide, 0.03% bromophenol blue (w/v), 0.03% xylene cyanol (w/v)) and boiled at 95 °C for 5 min. 10 µL of each reaction mixture was analyzed by electrophoresis on an 8M urea, 18% - polyacrylamide gel.

### M13 Forward Mutation Assay

The M13mp2 gap-filling forward mutation assay was performed as described previously<sup>21</sup>. Briefly, the gap-filling reaction (15 µL) was carried out in polymerase reaction buffer [25 mM Tris-HCl (pH 9.0), 1 mM DTT, 10 mM MgCl<sub>2</sub>, and 50 mg/mL BSA] containing 4 fmol of purified double-stranded bacteriophage M13mp2 DNA with a 407 nucleotide single stranded gap within the *lacZα*-complementation target sequence, 5 pmol of purified KPom1 or KPom1<sup>exo-</sup>, and 100 µM of each dNTP. Reactions were incubated at 37 °C for 10 min and were terminated by the addition of EDTA to a concentration of 10 mM. The completion of gap-filling reactions was confirmed by agarose gel electrophoresis. Aliquots of gap-filling reactions were transformed into MC1061 cells and plated on agar plates containing X-gal (5-bromo-4-chloro-3-indolyl-β-D-galactoside), IPTG (Isopropyl β -D-1-thiogalactopyranoside), and a lawn of CSH50 *E. coli* host cells. After incubation of plates at 37 °C for 16 h, the number of wild-type (dark blue) and mutant (light blue and white) plaques were scored. Mutant plaques were isolated and individually grown in liquid culture, and the M13mp2 DNA was isolated and sequenced using the sequencing primer 5'-TCGGAACCACCATCAAAC-3'. Error rates were calculated as previously described<sup>14</sup>.

### Single Nucleotide Insertion Kinetics

The primer extension reaction was performed to determine single nucleotide insertion kinetics as described previously<sup>15; 16</sup>. Briefly, the 5'-[<sup>32</sup>P]-labeled 16-mer primer : 5'-CATGAACTACAAGGAC-3' was annealed to a 1.5-fold molar excess of the template 36-mer : 5'-GCATTCAGT**X**GTCTTGTAGTTCATG-3', where the bold 'X' was either A, C, T, or G. Primer extension reactions (40 µL) were carried out in polymerase reaction buffer [25 mM Tris-HCl (pH 9.0), 1 mM DTT, 10 mM MgCl<sub>2</sub>, and 50 mg/mL BSA], containing 10 nM <sup>32</sup>P-labeled primer/template DNA, 20 nM of purified KPom1<sup>exo-</sup> and indicated concentrations of dNTPs. Reactions were incubated at 37 °C ranging for 1 to 15 min. The time of each reaction was chosen based on prior experiments that were performed to determine single completed hit conditions with less than 20% of total primer extended<sup>16; 17</sup>. Reactions were terminated by adding 40 µL of 2× gel loading buffer [95% formamide, 15 mM EDTA, 0.05% (w/v) bromophenol blue, and 0.05% (w/v) xylene cyanol]. Samples were

boiled and loaded onto an 8M urea, 15% -polyacrylamide gel for analysis by electrophoresis.

## Results

### KPom1 can substitute for DNA polymerase Pol I in *E. coli*

KPom1 is a member of the A-family of DNA polymerases. There is a high degree of conservation of amino acid sequences at the catalytic sites of DNA polymerases; sequence alignment of KPom1 with *E. coli* Pol I shows that all the required motifs for polymerase activity in Pol I are present in KPom1 and are highly conserved (Fig. 1B). We have previously shown that both mammalian Pol  $\beta$ <sup>18</sup> and HIV reverse transcriptase<sup>19</sup> can complement *E. coli* harboring a temperature sensitive mutation in Pol I<sup>18; 19</sup>. To determine whether KPom1 can substitute for *E. coli* Pol I, KPom1 was inserted into an IPTG inducible vector and transformed into *E. coli* that expresses a temperature-sensitive variant of Pol I (Pol I<sup>ts</sup>). At 37 °C, Pol I<sup>ts</sup> is inactivated and the strain is dependent upon an exogenously supplied polymerase for colony formation. Figure 2A and 2B demonstrate that KPom1 almost fully restores wild-type growth when induced with IPTG. In the absence of IPTG, the KPom1 containing plasmid fails to form colonies at the non-permissive temperature. In addition, essentially no growth is observed in the vector only control or when cells are transformed with a copy of KPom1 harboring an active site mutation, D1798A, that inactivates the polymerase (Fig. 2A,B).

### KPom1 is error prone *in vivo*

We took advantage of the ability of KPom1 to substitute for the endogenous Pol I activity of *E. coli* in order to determine its *in vivo* fidelity. We utilized a two-plasmid system detailed by Camps et al that uses a bacterial host that is Pol I<sup>ts</sup> (Figure 3 A)<sup>12; 18</sup>. In this system, one plasmid encodes the polymerase of interest (Klenow fragment of Pol I or KPom1 and its exonuclease deficient derivatives), while the other contains the  $\beta$ -lactamase gene with an ochre (TAA) mutation. Any mutations that result in a reversion of the ochre codon will lead to active  $\beta$ -lactamase activity and carbenicillin resistance. Thus, the frequency of bacteria rendered carbenicillin resistant reflects the frequency of ochre codon mutagenesis in the target plasmid.

Figure 3B shows the results for the *in vivo* reversion of mutations in  $\beta$ -lactamase by Klenow, Klenow<sup>exo-</sup>, KPom1, and KPom1<sup>exo-</sup>. The reversion frequencies for Klenow and Klenow<sup>exo-</sup> are consistent with previous reports on  $\beta$ -lactamase reversion with this system<sup>12</sup>. Specifically, the reversion frequency with Klenow<sup>exo-</sup> is 4.5-fold greater than that observed with exonuclease proficient Klenow and is consistent with previous reports<sup>12; 20</sup>. In JS200 strains expressing the KPom1 and KPom1<sup>exo-</sup> enzymes, the reversion frequency is much higher than that of the corresponding controls. The KPom1 enzyme exhibits a 9-fold higher reversion frequency than the Klenow fragment of *E. coli* Pol I. Surprisingly, KPom1<sup>exo-</sup> exhibits a 793-fold increase in the *in vivo* reversion frequency relative to *E. coli* Pol I<sup>wt</sup> and 41-fold higher than KPom1 (Fig. 3B) and suggests that the polymerase domain of KPom1 is very error prone and that the majority of polymerase mistakes are corrected by the exonuclease domain of the enzyme in the context of this system. Interestingly, the extremely high reversion frequency by KPom1<sup>exo-</sup> occurs in the context of the A/T rich TAA ochre codon and that the plDNA genome that this enzyme replicate is also A/T rich.

### Biochemical characterization of KPom1

In order to determine if KPom1 exhibits lower fidelity for nucleotide mis-insertions opposite template dA or dT relative to template dC or dG we used the purified enzyme to measure the *in vitro* fidelity and incorporation kinetics for all 16 possible base-pairs. We were unable to

express the apicoplast DNA polymerase in *E. coli* or yeast using different high expression vectors. We reasoned that this lack of high expression could be due to the disparity in the codon usage bias between *P. falciparum* and *E. coli*. Therefore, we obtained a chemically synthesized gene, optimized for *E. coli* and coding for the amino acids 1431-2016 of Pfp<sub>prex</sub> (Supplemental Fig. S1), which corresponds to the Pol I-like DNA polymerase domain (KPom1). The expressed N-terminal maltose binding domain fusion protein was purified to near homogeneity using a heparin column followed by amylose resin (Supplemental Fig. S2). After cleavage and removal of the maltose binding peptide, the purified DNA polymerase is highly active, with a specific activity of 77 pmoles of dNMPs incorporated per minute per ng of protein for KPom1<sup>WT</sup> and 53 pmoles/min-ng for KPom1<sup>exo-</sup>. KPom1 exhibits maximal activity at ~10mM Mg<sup>+2</sup> (Supplemental Fig. S3A) and pH 9.0 (Supplemental Fig. S3B). Polymerase activity increases 2-fold from 18 to ~40°C and then rapidly declines; consistent with the idea that enzyme activity has evolved for DNA replication in warm-blooded animals (Supplemental Fig. S3C).

### Fidelity of DNA Synthesis by KPom1 DNA Polymerase

The fidelity of DNA synthesis by the wild-type and exonuclease-deficient KPom1 DNA polymerases was determined using the M13mp2 forward mutation assay<sup>21</sup>. The substrate is double-stranded M13mp2 with a 407 nucleotide single-stranded gap in the *LacZα* gene. A purified DNA polymerase is used to fill in the single stranded segment *in vitro*, which is then transformed into *E. coli* and plated on a lawn of *α*-complementation cells in the presence of X-gal and IPTG. Accurate synthesis by the polymerase results in faithful replication of the *LacZα* gene and the formation of dark blue plaques, while polymerase errors yield light blue or colorless plaques. The fidelity of the polymerase is determined from the ratio of mutant to wild-type plaques; the error spectrum of the polymerase is determined by sequencing the resulting plaques. This assay allows for the monitoring of a broad range of mutations, including all 12 single-nucleotide misinsertion mutations and small insertion-deletion mutations, as well as short duplications, additions and rearrangements<sup>21</sup>. With the 'wild-type' KPom1, only 14 phenotypic colonies (i.e. light blue or colorless plaques) were observed in the 10,769 observed colonies, resulting in a mutation frequency of 0.13%; less than 2-fold greater than the background of the assay of 0.07%<sup>20; 21</sup>. In contrast, with KPom1<sup>exo-</sup>, 114 mutant plaques were detected in a total of 18,254 plaques, resulting in a mutation frequency of 0.63%. These mutation frequencies for both the wild-type and exonuclease deficient KPom1 are similar to those observed for other high fidelity A-family polymerases, including *E. coli* Pol I<sup>20</sup>, *Taq* DNA polymerase<sup>22</sup>, and human DNA polymerase  $\gamma$ <sup>23</sup>. The presence of the exonuclease domain imparts at least a 6-fold increase in the fidelity, thus showing that it is able to correct most misincorporation events that the polymerase active site makes.

The error spectrum of KPom1 was determined by sequencing the observed *lacZ* mutants and tabulating the types and sequence contexts of the mutations. The results for both KPom1<sup>wt</sup> and KPom1<sup>exo-</sup> were used to calculate the error rates for each type of mutation (Fig. 4 and Table 1), and the error spectrum of the KPom1<sup>exo-</sup> was compared to that of other characterized polymerases (Table 2). For KPom1<sup>exo-</sup>, 39 of the 115 sequenced verified mutants were single-base insertion or deletions; the error rate was  $1.2 \times 10^{-5}$  and  $0.2 \times 10^{-5}$ , respectively. Of the 34 detected -1 frameshift mutations found, 28 were in nucleotide repeats of two or more identical bases, which is consistent with a mechanism involving a template slippage event<sup>24</sup>.

For KPom1<sup>exo-</sup>, 69 of the 115 phenotypic mutants consisted of single-base substitutions, a base substitution error rate of  $3.9 \times 10^{-5}$ . Even though the M13mp2 forward mutation assay can detect all of the 12 single-base substitutions, only a subset were observed. Of the 69 sequenced single-base substitutions, the majority (52/69 or 75%) were the result of a T→C

transition (i.e. T:dGMP). The frequency of this transition mutation was  $14 \times 10^{-5}$ ; three-times greater than the frequency generated by the closely related *E. coli* Pol I<sup>exo-</sup> (Fig. 4, Table 1 and 2)<sup>20</sup>. The second most common observed base-substitution (10/69 or 14%) was the G→A (i.e G:dTMP) transition, which occurs at a rate of  $3.2 \times 10^{-5}$ ; six-fold higher than what is observed for *E. coli* Pol I<sup>exo-</sup><sup>20</sup>. Both the C→T (C:dAMP) and A→G (A:dCMP) mutations occur at a rate of  $1.1 \times 10^{-5}$  and, combined, only account for 10% of the observed single base substitutions. No other base substitutions were observed. This error spectrum deviates significantly from *E. coli* Pol I<sup>exo-</sup>, even though these two enzymes share significant sequence identity in their active site motifs (Fig. 1B) and have a similar overall error rate. Specifically, KPom1<sup>exo-</sup> catalyzes primarily T→C transitions, while *E. coli* Pol I<sup>exo-</sup> misincorporations results predominantly in C→T transitions, and G→T and G→C transversions<sup>20</sup>. In addition, a majority of T→C mutations (~65%) with KPom1<sup>exo-</sup> DNA polymerase occurred in a sequence context in which the 5'-template base is either a C or a G. The mutation spectrum for KPom1<sup>exo-</sup> is most similar to that of the A-family lesion bypass polymerase, pol v (See discussion for details).

### Steady-state kinetics of KPom1

Examining the fidelity of KPom1 using steady-state kinetics gives an indication of which step in nucleotide discrimination process is rate limiting for the incorporation of specific deoxynucleoside triphosphates. For example, a higher  $K_m$  would suggest that nucleotide discrimination is due to an increase in substrate dissociation (increase in  $k_{off}$ ), while a lower  $V_{max}$  would indicate an unfavorable geometry of the bound nucleotide in the active site<sup>16;20</sup>. We used a steady-state gel-based assay to determine the apparent kinetic parameters ( $V_{max}$  and  $K_m$ ) for the incorporation of the correct or incorrect nucleotide across for all 16 possible base pairings. These values were then used to calculate the fidelity of KPom1<sup>exo-</sup><sup>16</sup>.

KPom1<sup>exo-</sup> efficiently incorporated dAMP, dCMP, dTMP, or dGMP across from their complementary template bases and discriminated against the incorrect nucleotide for all possible nucleotide mismatches (Table 3). The calculated values for the fidelity of nucleotide misinsertion range from  $4.6 \times 10^{-3}$  (T:dGMP) to  $2.6 \times 10^{-5}$  (A:dCMP) (Table 3). Values for some mismatches could not be calculated due to the lack of observable incorporation. The most prevalent mis-insertions observed in the kinetic assay are the same as the mispairs with the lowest observed fidelity in the M13mp2 forward mutation assay (Table 1). The apparent values for  $K_m$  ranged from a 325- to 3000-fold increase for incorrect vs correct incorporation, but did not vary substantially for the correct incorporation reactions. The mispairs that were the least frequent in the M13mp2 forward mutation assay also exhibited a relatively high values for  $K_m$  ( $>1000 \mu M$ ), whereas base mispairs with the lowest fidelity tended to have much lower values of  $K_m$ . Specifically, the values for  $K_m$  were the highest when the identity of the template base was dG or dC or when base-pairing involved an incoming nucleotide with the same identity as the template base. Conversely, when the template base was dA or dT, the values of  $K_m$  were on the order of 2-3 fold lower than values observed for dG or dC. This observation suggests that KPom1 uses a mechanism whereby nucleotide discrimination for certain base:base mispairs (namely template dG, template dC, and pyr:pyr/pur:pur) involves poor binding (i.e. increased off-rate).

In contrast to the values of  $K_m$ , which exhibit an increase in magnitude for all mismatches relative to the correct base pair, the values for the apparent  $V_{max}$  ranged from a 13.7-fold decrease to a 1.5-fold *increase* for incorrect vs correct incorporation. The apparent  $V_{max}$  for the correct incorporation reactions were very similar to one another, regardless of the template base identity, while the  $V_{max}$  for most mismatch reactions varied in a range of about 4-fold regardless of the identity of the template base. A notable exception is the T:dGMP mispair, which, surprisingly, exhibits a higher  $V_{max}$  than the correct base-pair.

Taken together, it appears that, depending on the template base identity, KPom1 uses two different strategies for nucleotide discrimination. When the identity of the template base is dG or dC, the polymerase primarily discriminates between the correct vs incorrect nucleotide based on reduced occupancy of the active site (i.e. the rate of dissociation is much faster than the rate of incorporation). This is most likely due to the inability of these mispairs to form stable hydrogen bonds between the template and the substrate. This is consistent with the idea that fidelity for template dG and dC is mostly governed by substrate dissociation. However, this observation is not the case for the G:dTMP mispair, which exhibits a reduced  $K_m$  while the value of  $V_{max}$  for this mismatch is unchanged relative to the other mispairs. This observation suggests that for this base mismatch, the fidelity is increasingly governed by the rate of product formation.

Interestingly, when the template base identity is dA or dT, the values of  $K_m$  tend to be much lower than that of dG or dC and only vary by less than two-fold, while the  $V_{max}$  exhibits a greater than 20-fold variation (Table 3). This observation is consistent with the fidelity of mismatches involving template dA or dT being governed mostly by the base-pair geometry in the polymerase active site. As mentioned previously, the T:dGMP base-pair has a higher  $V_{max}$  than the correct base-pair (Table 3) and indicates that the  $V_{max}$  for this mismatch does not contribute favorably to the fidelity and that the increased fidelity is primarily due to substrate dissociation.

## Discussion

Pfprex is a multi-functional fusion protein targeted to the apicoplast. Even though definitive proof is lacking, it is believed to be responsible for the replication of the apicoplast genome using a DNA Pol I-like domain. In addition, it may also function in apicoplast DNA repair and other DNA synthetic functions. Thus, its presence in the apicoplast is somewhat reminiscent of mammalian DNA polymerase  $\gamma$ , which is also nuclearly encoded and has been shown to carry out a variety of DNA synthetic functions in mitochondria. Because the apicoplast is a unique and required component of the malarial parasite, it could serve as an important target for specifically preventing or treating infections by the malaria parasite. To this end, we have expressed and purified, and present fidelity and kinetic studies of KPom1, the plastid targeted replicative DNA polymerase domain from the malarial parasite *P. falciparum*. Our results show that the polymerase domain of the apicoplast genome replication enzyme replicates the genome with high fidelity and has an overall fidelity similar to other fidelity A-family polymerases. The high level of fidelity stems from efficient discrimination of mismatch nucleotides at the active site, as well as the presence of a 3'→5' exonuclease domain involved in proofreading, which is efficient at removing the vast majority of mutations caused by mis-insertion at the active site.

Characterization of the exonuclease deficient form of KPom1 reveals the 'spectrum' of errors introduced by the polymerase. The frequencies of insertions and deletions (indels) of only a few nucleotides in length are similar to the evolutionarily related *E.coli* DNA Pol I<sup>exo-</sup>, as well as other high fidelity A-family polymerases<sup>20; 23</sup>. The finding that these indels occur at nucleotide repeats suggests that these mutations may be the result of a strand slippage event<sup>24</sup>. In addition to indels, single-base substitutions at specific template positions may also be caused by a strand slippage. The M13mp2 forward mutation assay show that a majority of the observed T→C mutations occur after a template dG or a dC. Slippage events could lead to a transient template misalignment with the template dG or dC remaining in the catalytic site followed by incorporation of the 'correct' nucleotide (i.e. dCMP and dGMP, respectively). Such a mechanism has been suggested to occur for human pol  $\gamma$ <sup>24</sup>



One of the most intriguing aspects of the KPom1 polymerase is the error spectrum for single base substitutions. The most frequent mutations observed with both Klenow<sup>exo-</sup> and KPom1<sup>exo-</sup> are T→C transitions; however, the error frequency for T→C transitions is more than three-fold greater during copying with KPom1. The next most frequently scored mutation for KPom1 is the G→A, while with *E. coli* DNA Pol I<sup>exo-</sup>, C→T and G→C mutations are the next most frequent base-substitutions<sup>20</sup>. The active site motifs in the polymerase sites for KPom1 and *E. coli* DNA Pol I are nearly identical, as is the overall accuracy in DNA synthesis; therefore, in order to account for the differences in the error spectrum, it is likely that distant amino acids have a profound effect on the types of misincorporations catalyzed at the polymerase site.

Of the DNA polymerases that have been analyzed using the M13mp2 forward mutation assay, the error spectrum of KPom1<sup>exo-</sup> most closely resembles that of human pol  $\nu$ , an error-prone lesion bypass polymerase that lacks a proof-reading exonuclease activity<sup>25</sup>. While the frequency of misincorporation by human pol  $\nu$  is greater than KPom1<sup>exo-</sup> (Table 2), pol  $\nu$  makes primarily G→A (G:dTMP) mutations, followed by the T→C (T:dGMP) substitutions<sup>25</sup>. In contrast, for KPom1, the primary mutations are T→C mutations followed by G→A substitutions. When considering the flanking sequence immediately 5' to a mutation, it is interesting to note that G→A mutations by pol  $\nu$  are primarily preceded by a template dA or dT, while the T→C mutation of KPom1 is primarily preceded by a template dG or dC. These observations suggest that the interaction of a polymerase with the template DNA must also influence the incorporation of specific incorrect nucleotides.

The apicoplast genome base-pair composition is >86% A/T<sup>4</sup> yet, the most frequent mutations produced by KPom1 are T→C transitions, both in the presence or absence of exonuclease activity. This finding would suggest that a genome with a higher G/C content would evolve over time, thus leading to an apicoplast genome with reduced A/T content. One possible explanation as to why a G/C bias is not observed may involve biased nucleoside pools within the parasite. *In vivo* studies have previously shown that the levels of adenosine and thiamine nucleosides are several times higher in the malarial parasite than are cytosine and guanine<sup>26</sup> and studies have shown that, on a genomic level, there is a distinct trend in the mutational bias towards high A/T content in bacterial obligate endosymbiotes and parasites<sup>27; 28</sup>. This enzyme may have evolved to lower the  $K_m$  value for dGTP and dCTP due to their reduced availability in the pool. This idea is consistent with our observations that mispairs involving dGTP and dCTP tend to have a lower  $K_m$ . Therefore, the skewed mutational bias exhibited by KPom1 may be the result of a selective advantage that keeps the A/T content of the genome from becoming too skewed and reducing organismal fitness. An alternative possibility as to why a G/C bias is not observed is that the misincorporation bias at the level of the DNA polymerase could be compensated for by a mismatch repair process that preferentially removes dGMP mismatches in the newly replicated DNA strand. However, we are unaware of evidence for a mismatch repair system that functions in apicoplast DNA.

The unique error signature of KPom1 is a product of its specific structural features that govern fidelity. This begs the question as to why KPom1 has an error spectrum similar to human pol  $\nu$ , even though the amino acid sequence is more closely related to *E. coli* pol I? A comparison of all six conserved polymerase motifs of KPom1, *E. coli* Pol I, and human pol  $\nu$  show that there are no amino acids that are conserved between KPom1 and pol  $\nu$  that are not also conserved in *E. coli* Pol I (Fig. 1B). This suggests that these motifs are not the only ones that govern the substrate selection by DNA polymerases and that other structural features or amino acids in the enzyme are also likely to affect substrate selection. Indeed, several multi-amino acid insertions flanking these conserved motifs in human pol  $\nu$  and pol  $\theta$ , another A-family bypass polymerase, have been implicated in its reduced fidelity, which suggests that

the determinants of fidelity are not strictly confined to the conserved polymerase motifs<sup>29; 30; 31</sup>.

Finally, our finding that KPom1 complements the *in vivo* activity of Pol I in *E. coli* will allow us to exploit genetic complementation for both structure-function studies and drug screening. Genetic complementation has been shown to facilitate the screening of large libraries of DNA polymerase mutants with random nucleotides at designated positions. An analysis of mutants of KPom1 will be important in identifying amino residues that govern nucleotide selection and that account for the unique substrate specificity. These mutants can then be compared to other A-family polymerases, as described previously<sup>32; 33</sup>.

The ability to substitute KPom1 for Pol I brings about the feasibility of using *E. coli* as a vehicle for evaluating the potency of DNA polymerase inhibitors in a high throughput manner. Such a system has been used to sensitize *E. coli* to the antiviral compound AZT by complementing HIV-RT<sup>19</sup>. The uniquely biased error spectrum of the KPom1 polymerase suggests that nucleoside analogs could be developed that exploits this bias as a method of terminating apicoplast DNA synthesis. Since the T→C error rate of KPom1 is much higher than that of human pol δ or pol ε, the replicative DNA polymerases in the nucleus, the design of specific nucleoside analogs that take this fact into account will more specifically target the parasitic polymerase instead of the replicative polymerases, thus minimizing the incorporation into the host genome.

## Supplementary Material

Refer to Web version on PubMed Central for supplementary material.

## Acknowledgments

This work was supported by the National Institutes of Health R01CA115202, R01CA102029, and P01AG033061. We thank Eddie Fox and Sharath Balakrishna for their useful comments and discussion.

## References

1. Snow RW, Guerra CA, Noor AM, Myint HY, Hay SI. The global distribution of clinical episodes of *Plasmodium falciparum* malaria. *Nature*. 2005; 434:214–217. [PubMed: 15759000]
2. He HY, Shaw MK, Pletcher CH, Striepen B, Tilney LG, Roos DS. A plastid segregation defect in the protozoan parasite *Toxoplasma gondii*. *EMBO J*. 2001; 20:330–339. [PubMed: 11157740]
3. Stanway RR, Witt T, Zobiak B, Aepfelbacher M, Heussler VT. GFP-targeting allows visualization of the apicoplast throughout the life cycle of live malaria parasites. *Biol Cell*. 2009; 101:415–430. [PubMed: 19143588]
4. Wilson RJM, Denny PW, Preiser PR, Rangachari K, Roberts K, Roy A, Whyte A, Strath M, Moore DJ, Moore PW, Williamson DH. Complete Gene Map of the Plastid-like DNA of the Malaria Parasite *Plasmodium falciparum*. *J Mol Biol*. 1996; 261:155–172. [PubMed: 8757284]
5. Dahl EL, Rosenthal PJ. Apicoplast translation, transcription and genome replication: targets for antimalarial antibiotics. *Trends Parasitol*. 2008; 24:243–284. [PubMed: 18450514]
6. Kumar A, Tanveer A, Biswas S, Ram EVSR, Gupta A, Kumar B, Habib S. Nuclear-encoded DnaJ homologue of *Plasmodium falciparum* interacts with replication *ori* of the apicoplast genome. *Mol Microbiol*. 2010; 75:942–956. [PubMed: 20487289]
7. Ram EVSR, Kumar A, Biswas S, Kumar A, Chaubey S, Siddiqi MI, Habib S. Nuclear *gyrB* encodes a functional subunit of the *Plasmodium falciparum* gyrase that is involved in apicoplast DNA replication. *Mol Biochem Parasit*. 2007; 154:30–39.
8. Dahl EL, Rosenthal PJ. Multiple antibiotics exert delayed effects against the *Plasmodium falciparum* apicoplast. *Antimicrob Agents Chemother*. 2007; 51:3485–3490. [PubMed: 17698630]

9. Dahl EL, Shock JL, Shenai BR, Gut J, DeRisi JL, Rosenthal PJ. Tetracyclines specifically target the apicoplast of the malaria parasite *Plasmodium falciparum*. *Antimicrob Agents Chemother*. 2006; 50:3124–3131. [PubMed: 16940111]
10. Goodman CD, Su V, McFadden GI. The effects of anti-bacterials on the malaria parasite *Plasmodium falciparum*. *Mol Biochem Parasit*. 2007; 152:181–191.
11. Seow F, Sato S, Janssen CS, Riehle MO, Mukhopadhyay A, Phillips RS, Wilson RJM, Barrett MP. The plastidic DNA replication enzyme complex of *Plasmodium falciparum*. *Mol Biochem Parasit*. 2005; 141:145–153.
12. Camps M, Naukkarinen J, Johnson BP, Loeb LA. Targeted gene evolution in *Escherichia coli* using a highly error-prone DNA Polymerase I. *Proc Natl Acad Sci USA*. 2003; 100:9727–9732. [PubMed: 12909725]
13. Shinkai A, Loeb LA. *In vivo* mutagenesis by *Escherichia coli* DNA polymerase I Ile<sup>709</sup> in motif A functions in base selection. *J Biol Chem*. 2001; 276:46759–46764. [PubMed: 11602576]
14. Glick E, Anderson JP, Loeb LA. *In vitro* production and screening of DNA polymerase  $\eta$  mutants for catalytic diversity. *Biotechniques*. 2002; 33:1136–1144. [PubMed: 12449395]
15. Schmitt MW, Matsumoto Y, Loeb LA. High fidelity and lesion bypass capability of human DNA polymerase  $\delta$ . *Biochimie*. 2009; 91:1163–1172. [PubMed: 19540301]
16. Boosalis MS, Petruska J, Goodman MF. DNA Polymerase Insertion Fidelity - Gel assay for site-specific kinetics. *J Biol Chem*. 1987; 262:14689–14696. [PubMed: 3667598]
17. Creighton S, Bloom LB, Goodman MF. Gel fidelity assay measuring nucleotide misinsertion, exonucleolytic proofreading, and lesion bypass efficiencies. *Methods Enzymol*. 1995; 262:232–256. [PubMed: 8594351]
18. Sweasy JB, Loeb LA. Mammalian DNA polymerase  $\beta$  can substitute for DNA polymerase I during DNA replication in *Escherichia coli*. *J Biol Chem*. 1992; 267:1407–1410. [PubMed: 1730689]
19. Kim B, Loeb LA. Human immunodeficiency virus reverse transcriptase substitutes for DNA polymerase I in *Escherichia coli*. *Proc Natl Acad Sci USA*. 1995; 92:684–688. [PubMed: 7531338]
20. Bebenek K, Joyce CM, Fitzgerald MP, Kunkel TA. The fidelity of DNA synthesis catalyzed by derivatives of *Escherichia coli* DNA polymerase I. *J Biol Chem*. 1990; 265:13878–13887. [PubMed: 2199444]
21. Bebenek K, Kunkel T. Analyzing fidelity of DNA polymerases. *Meth Enzymol*. 1995; 262:217–232. [PubMed: 8594349]
22. Eckert KA, Kunkel TA. High fidelity DNA synthesis by the *Thermus aquaticus* DNA polymerase. *Nuc Acids Res*. 1990; 18:3739–3752.
23. Longley MJ, Nguyen D, Kunkel TA, Copeland WC. The fidelity of human DNA polymerase  $\gamma$  with and without exonucleolytic proofreading and the p55 accessory subunit. *J Biol Chem*. 2001; 276:38555–38562. [PubMed: 11504725]
24. Bebenek K, Kunkel TA. Streisinger revisited: DNA synthesis errors mediated by substrate misalignments. *Cold Spring Harbor Symp Quant Biol*. 2000; 65:81–92. [PubMed: 12760023]
25. Arana ME, Takata Ki, Garcia-Diaz M, Wood RD, Kunkel TA. A unique error signature for human DNA polymerase  $\nu$ . *DNA Repair*. 2007; 6:213–223. [PubMed: 17118716]
26. Dyke, Kv; Trush, MA.; Wilson, ME.; Stealey, PK. Isolation and analysis of nucleotides from erythrocyte-free malarial parasites (*Plasmodium berghei*) and potential relevance to malaria chemotherapy. *B World Health Organ*. 1977; 55:253–264.
27. Hershberg R, Petrov DM. Evidence that mutation is universally biased towards AT in bacteria. *PLOS Genet*. 2010; 6:e1001115. [PubMed: 20838599]
28. Mann S, Chen YPP. Bacterial genomic G + C composition-eliciting environmental adaptation. *Genomics*. 2010; 95:7–15. [PubMed: 19747541]
29. Arana ME, Seki M, Wood RD, Rogozin IB, Kunkel TA. Low-fidelity DNA synthesis by human DNA polymerase theta. *Nuc Acid Res*. 2008; 36:3847–3856.
30. Takata, Ki; Arana, ME.; Seki, M.; Kunkel, TA.; Wood, RD. Evolutionary conservation of residues in vertebrate DNA polymerase N conferring low fidelity and bypass activity. *Nuc Acid Res*. 2010; 38:3233–3244.

31. Hogg M, Seki M, Wood RD, Doublie S, Wallace SS. Lesion bypass activity of DNA polymerase  $\theta$  (POLQ) is an intrinsic property of the pol domain and depends on unique sequence inserts. *J Mol Biol.* 2011; 405:642–652. [PubMed: 21050863]
32. Loh E, Choe J, Loeb LA. Highly tolerated amino acid substitutions increase the fidelity of *Escherichia coli* DNA polymerase I. *J Biol Chem.* 2007; 282:1201–12209.
33. Patel PH, Loeb LA. DNA polymerase active site is highly mutable: Evolutionary consequences. *Proc Nat Acad Sci USA.* 2000; 97:5095–5100. [PubMed: 10805772]

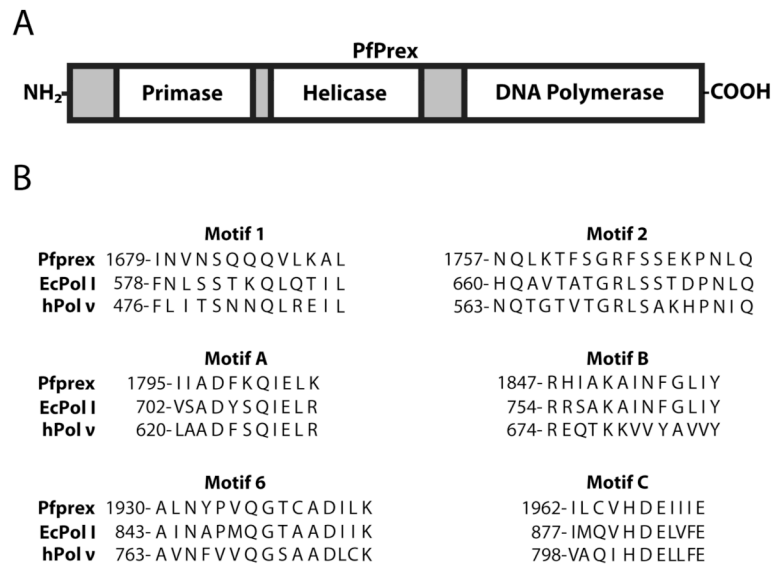


**Figure 1.** **A**, The domain organization of *Pfprex*. **B**, the sequence comparison of evolutionarily conserved DNA polymerase motifs of the *Plasmodium falciparum* *Pfprex* polymerase domain, *E. coli* DNA polymerase I, and human Pol v.

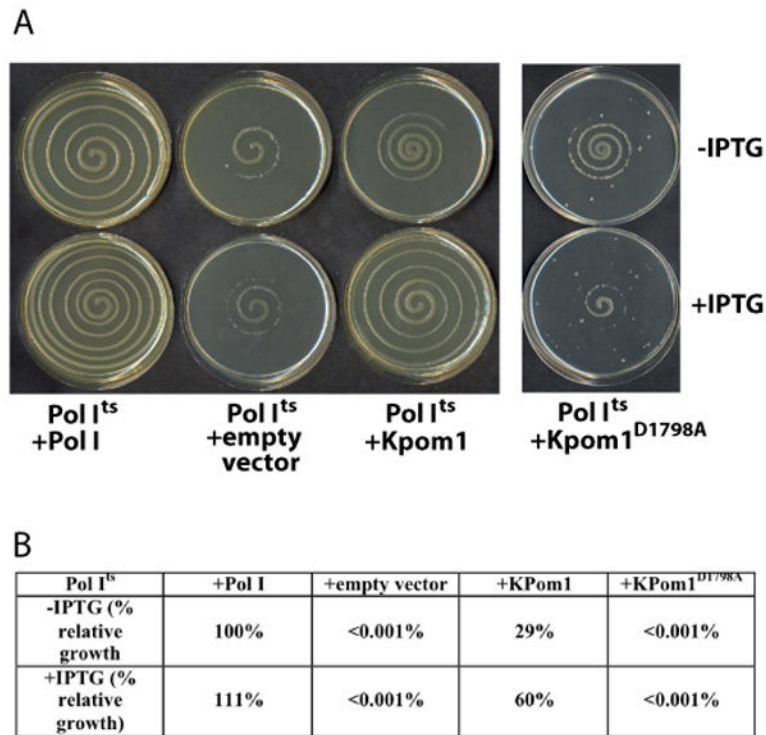


**Figure 2. Functional complementation of *E. coli* DNA polymerase I by *Plasmodium falciparum* KPom1 *in vivo***

(A) *E. coli* JS200 cells were transformed with an empty pHSG576 vector or vector harboring Pol I, KPom1 or KPom1<sup>D1798A</sup> gene. (B), The complementation efficiency of Pol I<sup>ts</sup> cells by exogenously expressed Pol I, KPom1 or KPom1<sup>D1798A</sup> were quantified as described in Camps *et al*<sup>12</sup>. The complementation efficiency of Pol I<sup>ts</sup> cells by KPom1 or KPom1<sup>D1798A</sup> was normalized to the conditions with Pol I in the absence of IPTG, which was set as 100%. Assays were done in triplicate.

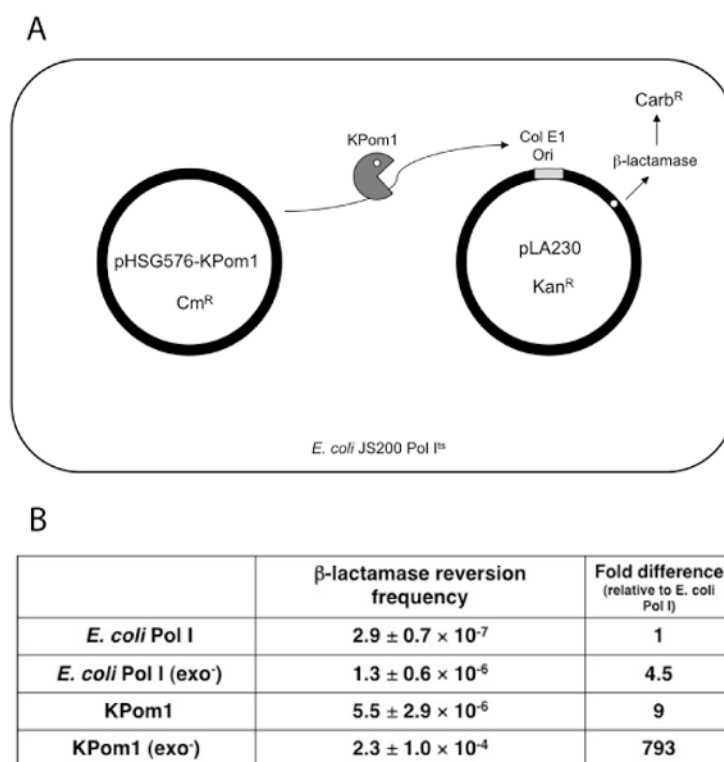


**Figure 3. *In vivo* fidelity of KPom1**

(A) Schematic diagram of the two-plasmid  $\beta$ -lactamase reversion assay. JS200 (Pol I<sup>S</sup>) cells were transformed with two plasmids. Plasmid pHSG576 is a low copy number plasmid and carries the *polA* gene under control of the *tac* promoter. The pLA230 plasmid carries the  $\beta$ -lactamase gene placed in close proximity downstream of a pUC19 (ColE1-type) origin of replication. The polymerase of interest is expressed from pHSG576 and initiates replication of pLA230. If the polymerase makes a misinsertion when copying the ochre codon, it will lead to a reversion a functional  $\beta$ -lactamase enzyme. (B) Reversion frequencies for the  $\beta$ -lactamase reversion assay. The fold-increase in the reversion frequency is relative to *E. coli* Pol I.





Table 1

Mutation rates in the *LacZ* forward mutation assay

Mismatch	#of Detectable Sites	Wild-Type			Exo <sup>c</sup>		
		Number Detected	Error Rate ( $\times 10^{-5}$ )	Number Detected	Error Rate ( $\times 10^{-5}$ )	Number Detected	Error Rate ( $\times 10^{-5}$ )
T•dTMP	16	0	$\leq 0.3$	0	$\leq 0.4$	0	$\leq 0.4$
T•dGMP	27	1	0.17	52	1.4	14	1.4
T•dCMP	23	0	$\leq 0.2$	0	$\leq 0.3$	0	$\leq 0.3$
C•dTMP	16	0	$\leq 0.3$	0	$\leq 0.4$	0	$\leq 0.4$
C•dAMP	25	2	0.36	4	1.1	4	1.1
C•dCMP	9	0	$\leq 0.5$	0	$\leq 0.8$	0	$\leq 0.8$
G•dTMP	22	0	$\leq 0.2$	10	3.2	10	3.2
G•dAMP	25	0	$\leq 0.2$	0	$\leq 0.3$	0	$\leq 0.3$
G•dGMP	19	0	$\leq 0.2$	0	$\leq 0.4$	0	$\leq 0.4$
A•dAMP	23	0	$\leq 0.2$	0	$\leq 0.3$	0	$\leq 0.3$
A•dGMP	17	0	$\leq 0.3$	0	$\leq 0.4$	0	$\leq 0.4$
A•dCMP	29	1	0.24	3	1.1	3	1.1
<b>Base Substitutions</b>	125	4	0.14	69	3.9	69	3.9
+ Insertions	199	0	$\leq 0.02$	5	0.2	5	0.2
-1 Deletions	199	6	0.14	34	1.2	34	1.2
Large Deletion <sup>a</sup>	Not Defined	4	25	7	37	7	37
<b><i>LacZ</i> mutation frequency</b>			$1.3 \times 10^{-3}$		$6.3 \times 10^{-3}$		$6.3 \times 10^{-3}$

<sup>a</sup>For large deletions, mutation frequency is reported instead of error rate.

**Table 2**  
**Comparison of mutation rates between KPom1<sup>exo-</sup> and other polymerases**

DNA polymerase	Single-base deletion error rate ( $\times 10^{-5}$ )	Single-base substitution error rate ( $\times 10^{-5}$ )
Kpom1 (exo) <sup>a</sup>	1.2	3.9
<i>E. coli</i> Klenow (exo) <sup>b</sup>	0.6	2.5
Taq pol (exo) <sup>c</sup>	0.6	1.7
hPol $\nu$ <sup>d</sup>	17	350
hPol $\theta$ <sup>e</sup>	140	240
hPol $\gamma$ (exo) (+p140 & p55) <sup>f</sup>	0.8	4.1
hPol $\alpha$ <sup>g</sup>	2.8	7.5
hPol $\delta$ (exo) <sup>h</sup>	2.0	4.4
$\gamma$ Pol $\epsilon$ (exo) <sup>i</sup>	5.6	24
hPol $\beta$ <sup>j</sup>	14	23
hPo $\lambda$ <sup>j</sup>	450	90
hPol $\eta$ <sup>k</sup>	240	3500
hPol $\kappa$ <sup>l</sup>	180	580

<sup>a</sup>Error rates are from this study.

<sup>b</sup>Single-base deletion are from Minnick *et al.*, 1996<sup>34</sup>; Single-base substitutions are from Bebenek *et al.*, 1990<sup>20</sup>.

<sup>c</sup>Error rates are from Eckert and Kunkel, 1990<sup>22</sup>.

<sup>d</sup>Error rates are from Arana *et al.*, 2007<sup>25</sup>.

<sup>e</sup>Error rates are from Arana *et al.*, 2008<sup>29</sup>.

<sup>f</sup>Single-base deletions are from Longley, *et al.*, 2001<sup>23</sup>; Single-base substitutions are reported in Table 2 of Arana *et al.*, 2007<sup>25</sup>.

<sup>g</sup>Error rates are unpublished data reported in Table 2 of Arana *et al.*, 2007<sup>29</sup>.

<sup>h</sup>Error rates are from Schmitt, *et al.*, 2009<sup>15</sup>.

<sup>i</sup>Error rates are from Shcherbakova, *et al.*, 2003<sup>35</sup>

<sup>j</sup>Error rates are from Bebenek, *et al.*, 2003<sup>36</sup>

<sup>k</sup>Error rates are from Matsuda, *et al.*, 2000<sup>37</sup> and Matsuda, *et al.*, 2001<sup>38</sup>

<sup>l</sup>Error rates are from Ohashi, *et al.*, 2000<sup>39</sup>.

**Table 3**  
**Fidelity of single nucleotide insertion by KPom1<sup>exo-</sup>**

Base pair	$K_m$ ( $\mu$ M)	$V_{max}$ (fmol/min)	$V_{max}/K_m^a$	Fidelity <sup>b</sup>
T•dAMP	1.6±0.7	12.5±0.7	7.8	1
T•dTMP	N.D. <sup>c</sup>	N.D. <sup>c</sup>	-	-
T•dGMP	521±54	18.8±0.6	0.0361	4.61×10 <sup>-3</sup>
T•dCMP	648±350	0.91±0.13	0.0014	1.80×10 <sup>-4</sup>
C•dGMP	0.36±0.09	8.2±0.4	22.8	1
C•dTMP	1300±450	0.81±0.09	.0006	2.74×10 <sup>-5</sup>
C•dAMP	N.D. <sup>c</sup>	N.D. <sup>c</sup>	-	-
C•dCMP	N.D. <sup>c</sup>	N.D. <sup>c</sup>	-	-
G•dCMP	0.72±0.09	10.4±0.3	14.4	1
G•dTMP	290±120	3.2±0.6	0.0110	7.64×10 <sup>-4</sup>
G•dAMP	1450±650	3.9±0.7	0.0027	1.86×10 <sup>-4</sup>
G•dGMP	2200±620	3.0±0.4	0.0014	9.44×10 <sup>-5</sup>
A•dTMP	0.70±0.15	11.4±0.6	16.30	1
A•dAMP	1500±260	1.6±0.2	0.0011	6.55×10 <sup>-5</sup>
A•dGMP	264±117	2.9±0.2	0.0110	6.74×10 <sup>-4</sup>
A•dCMP	885±228	0.92±0.15	0.0010	6.38×10 <sup>-5</sup>

<sup>a</sup>Units are reported in fmol/ $\mu$ M•min

<sup>b</sup>Fidelity is defined as  $(V_{max}/K_m)_{wrong}/(V_{max}/K_m)_{right}$

<sup>c</sup>The reaction was too slow to be determined